Supplemental Figure 1

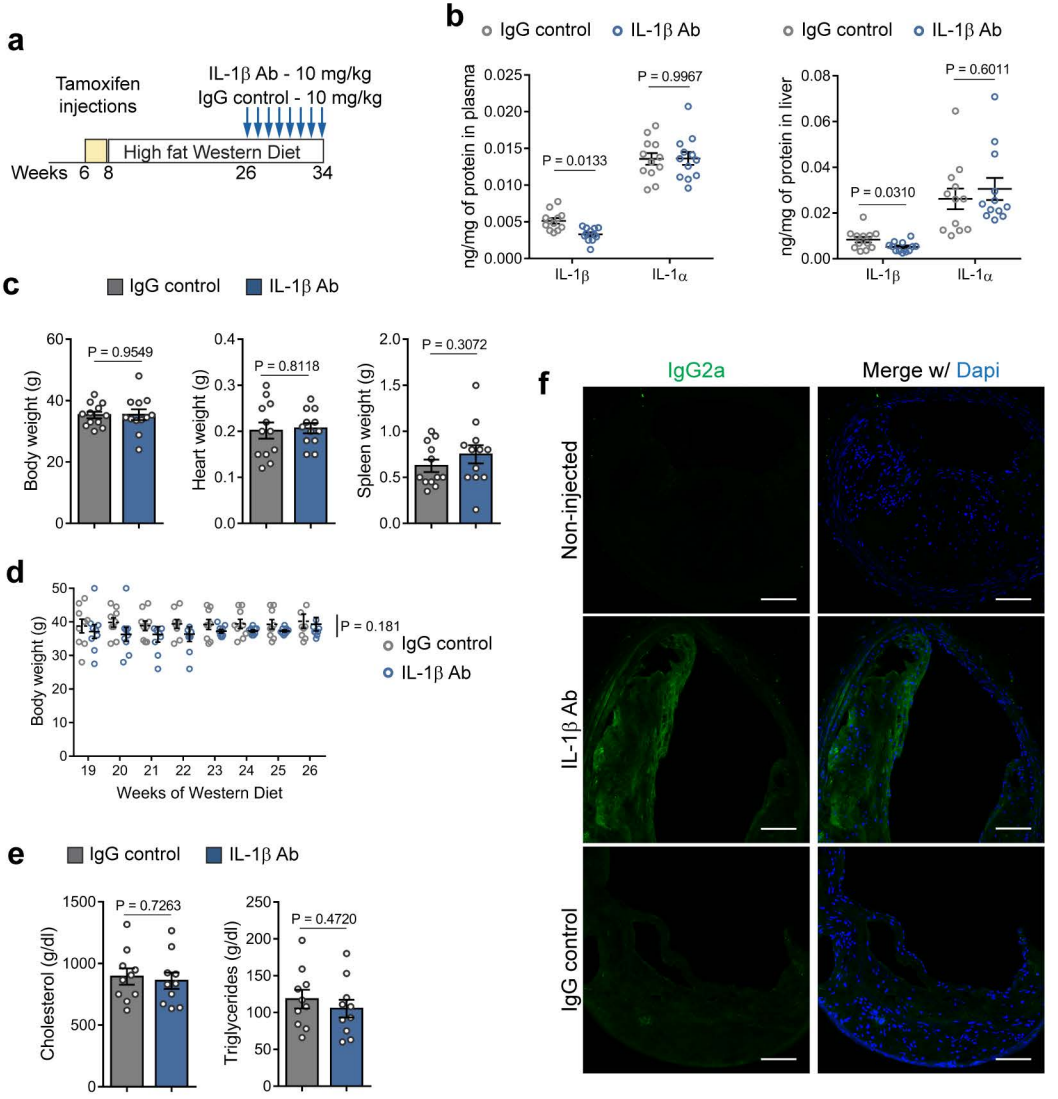

Supplemental Figure 2

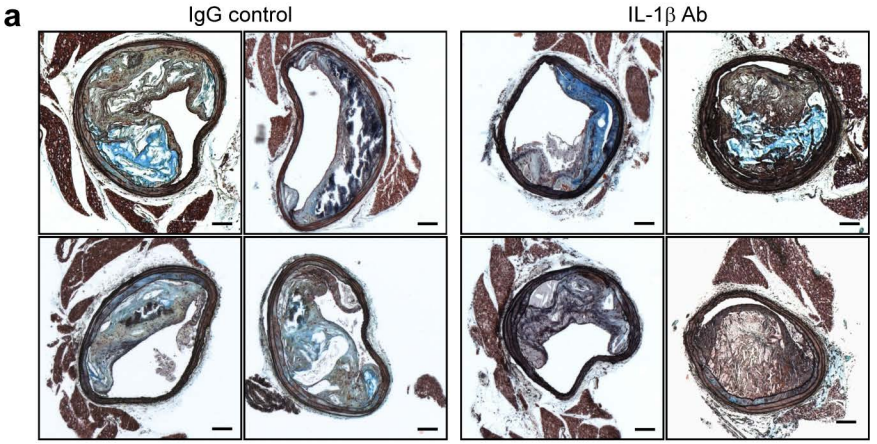

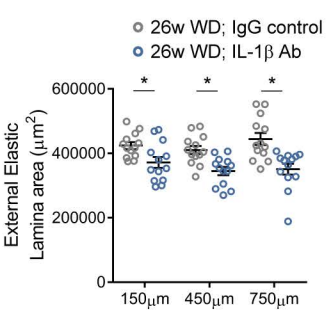

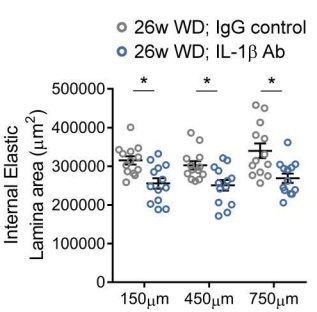

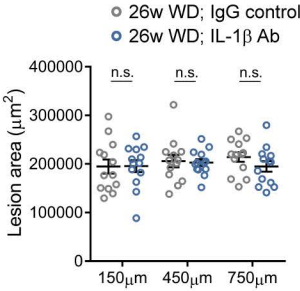

e

P values

Location	150μm	450μm	750μm
EEL	0.0455	0.0088	0.0076
IEL	0.080	0.0255	0.0013
Lesion	0.999	0.996	0.559

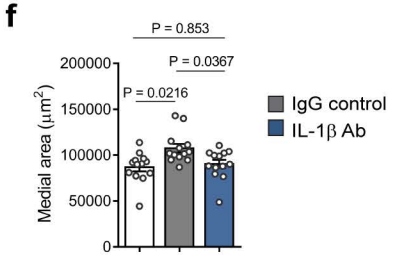

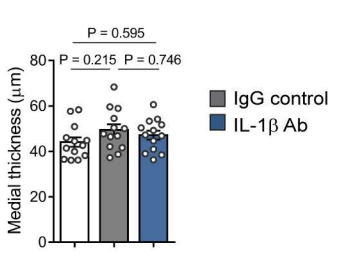

Supplemental Figure 3

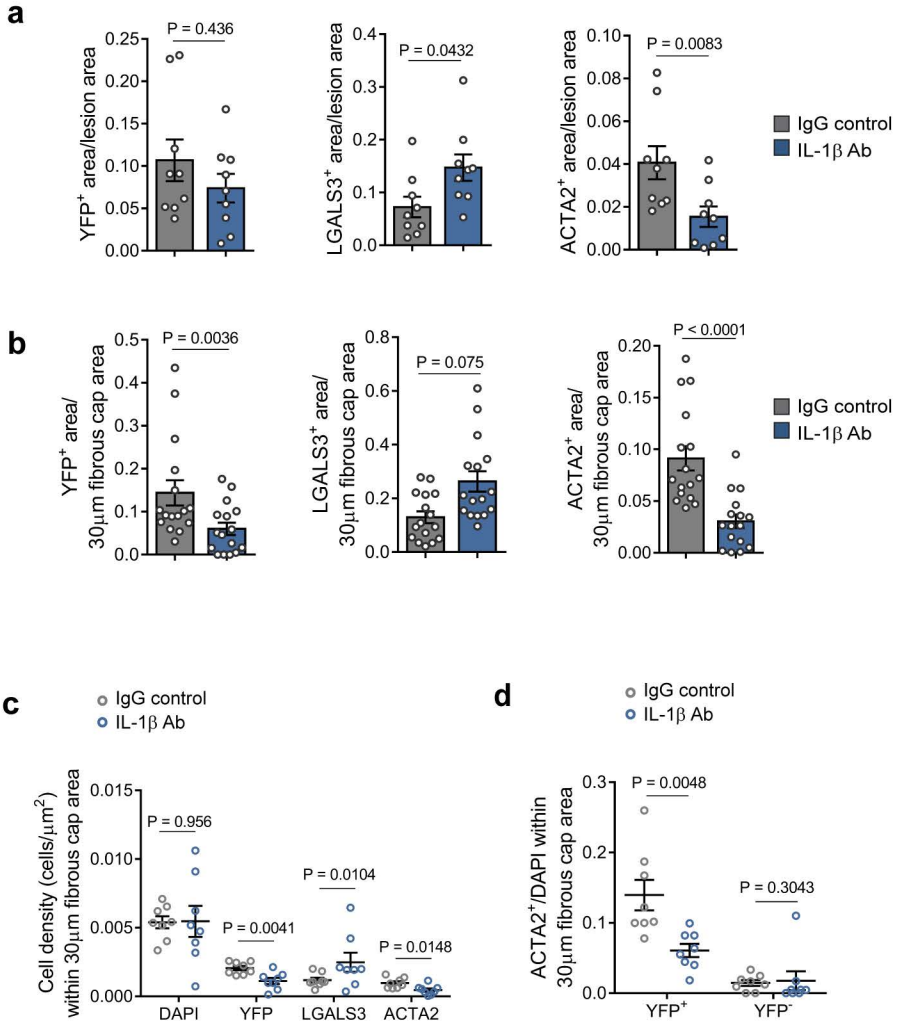

Supplemental Figure 4

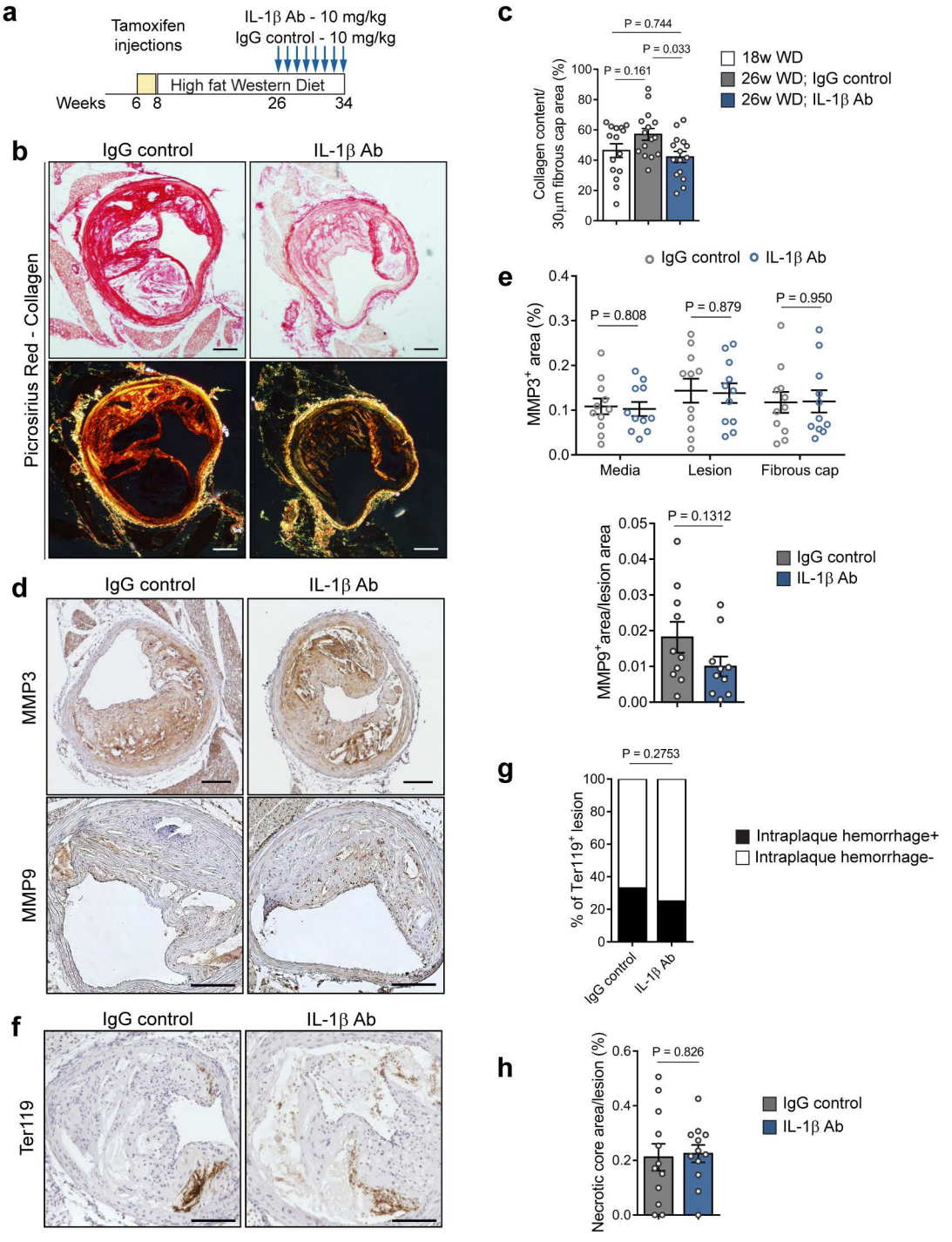

Supplemental Figure 5

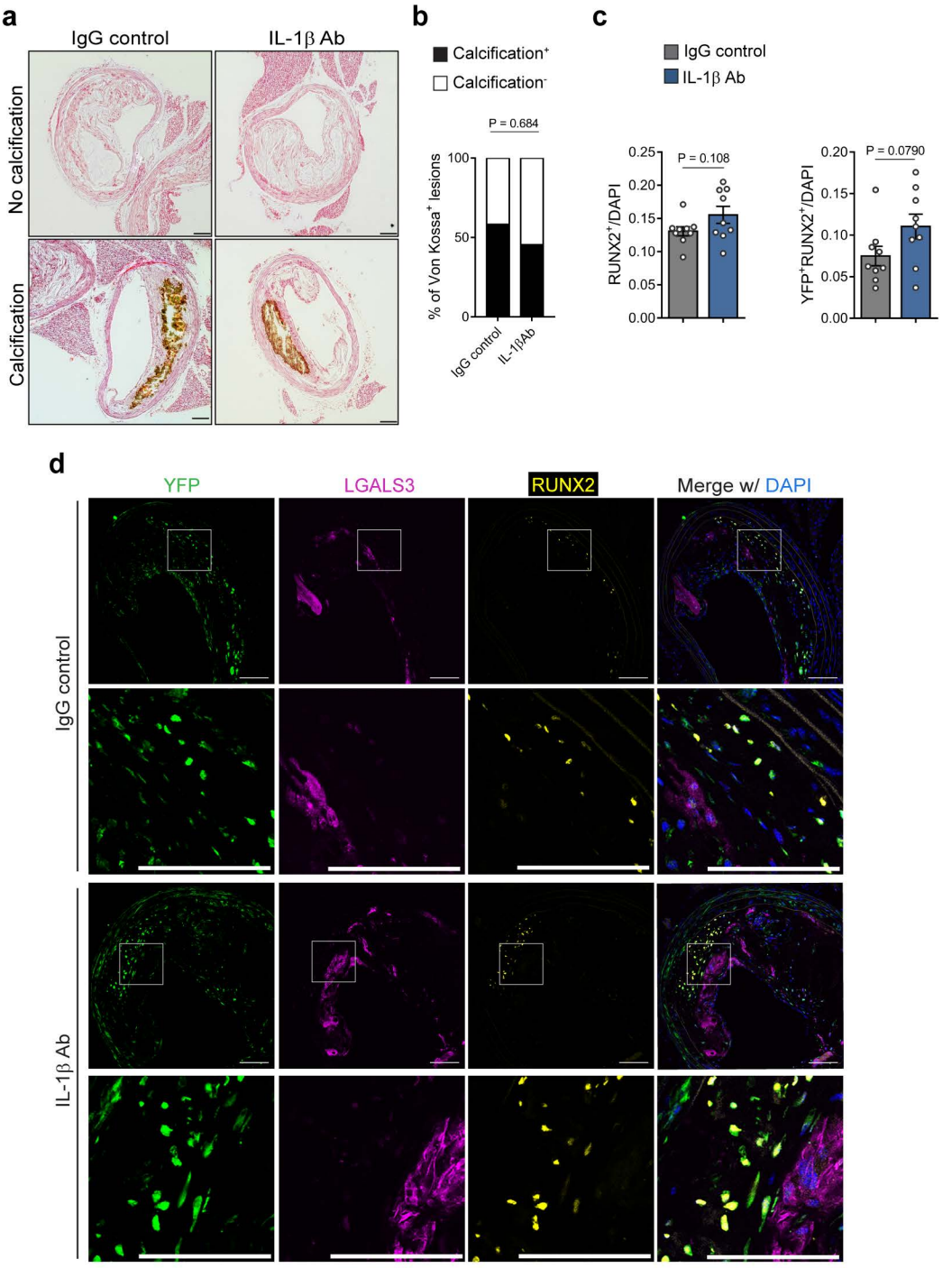

Supplemental Figure 6

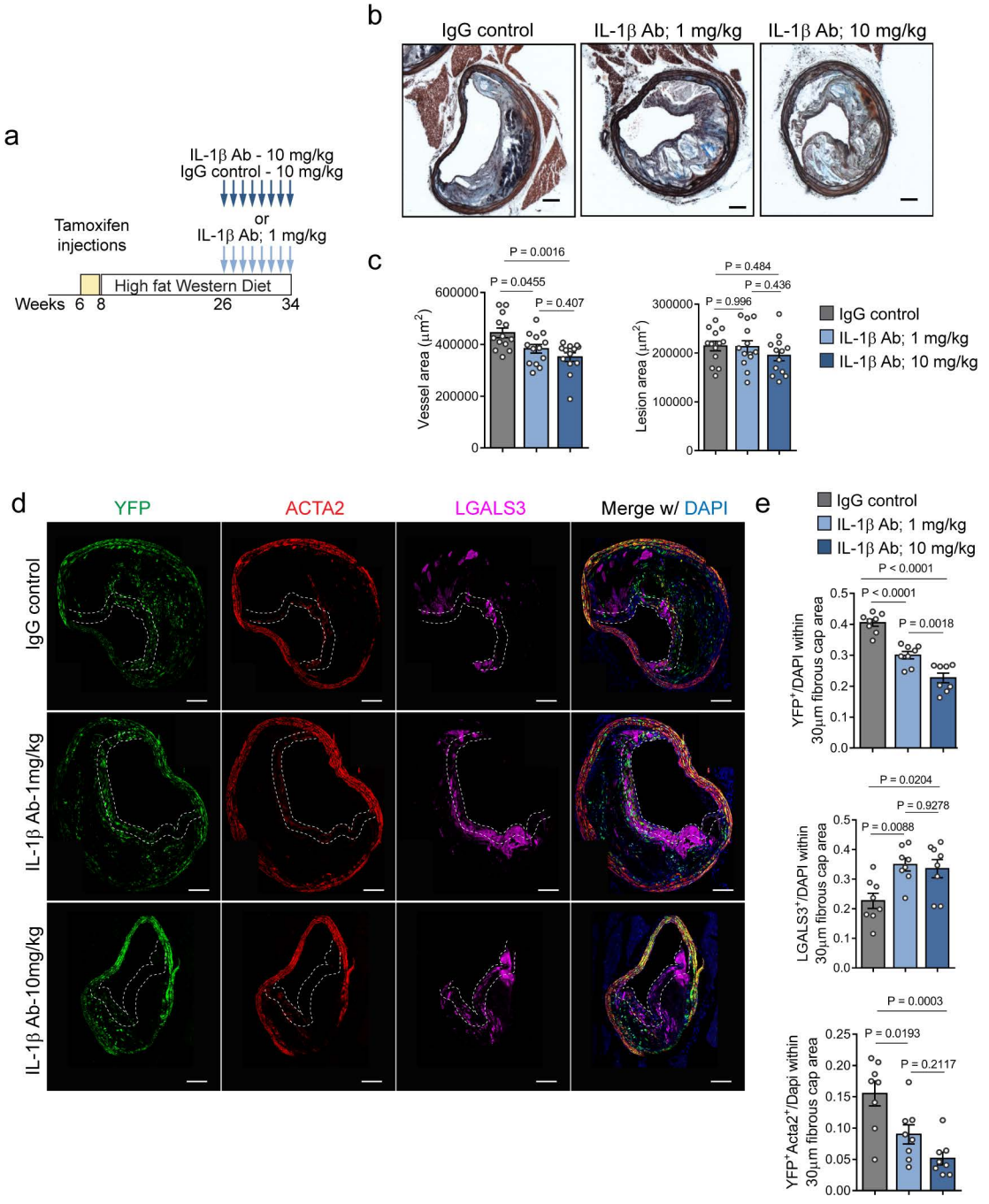

Supplemental Figure 7

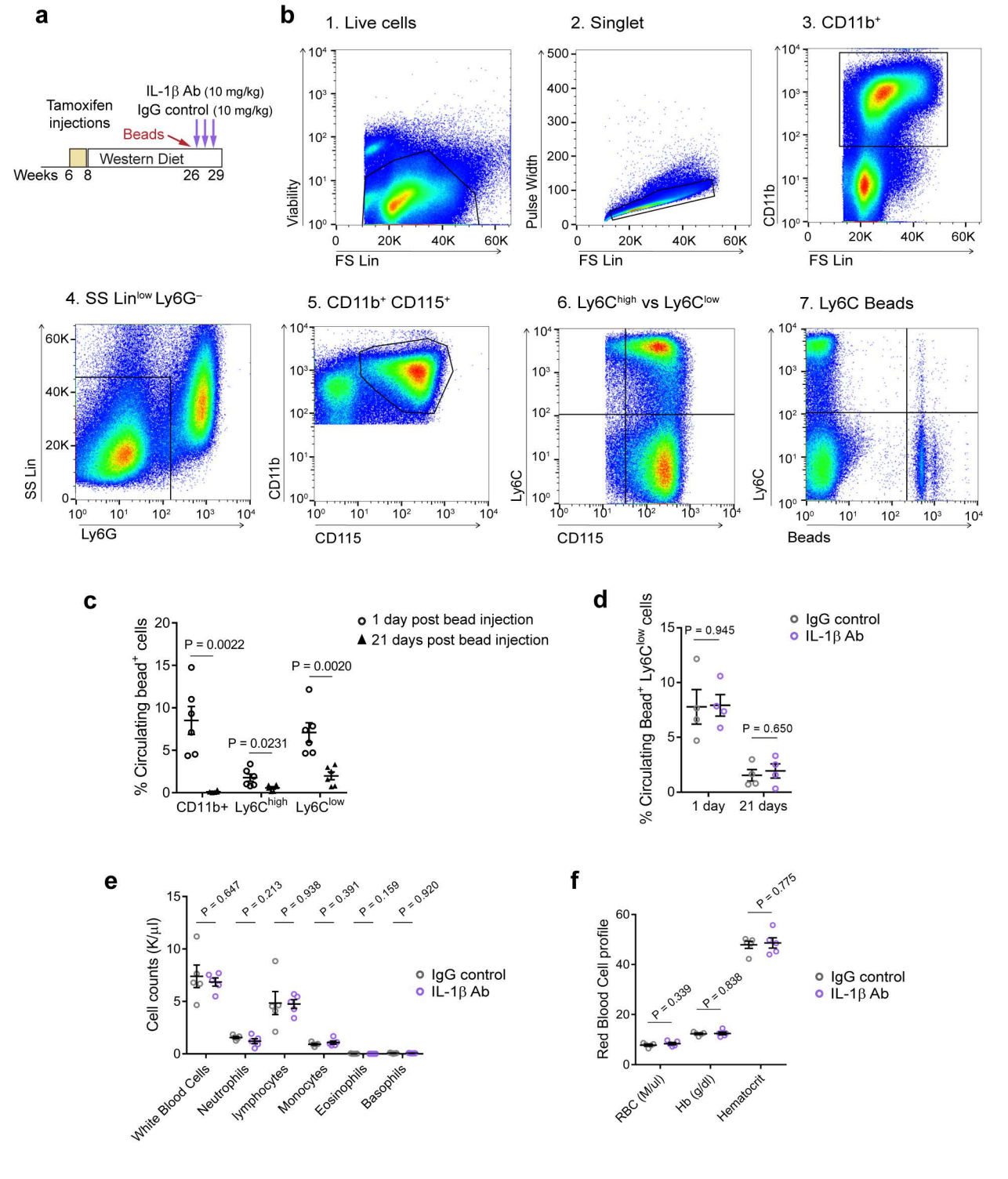

Supplemental Figure 8

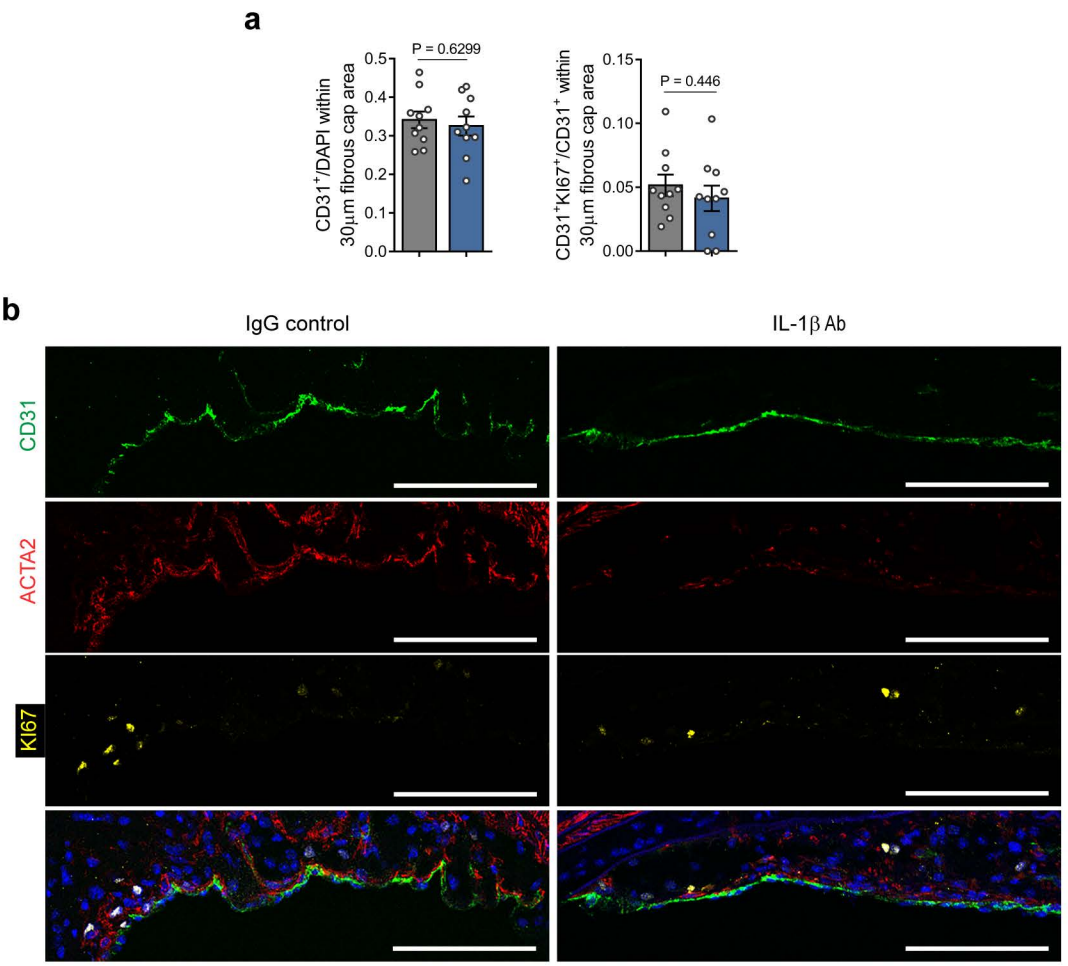

Supplemental Figure 9

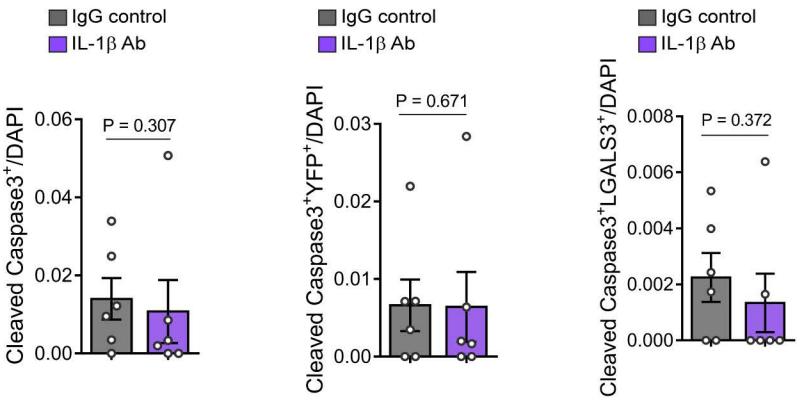

Supplementary Figure 10

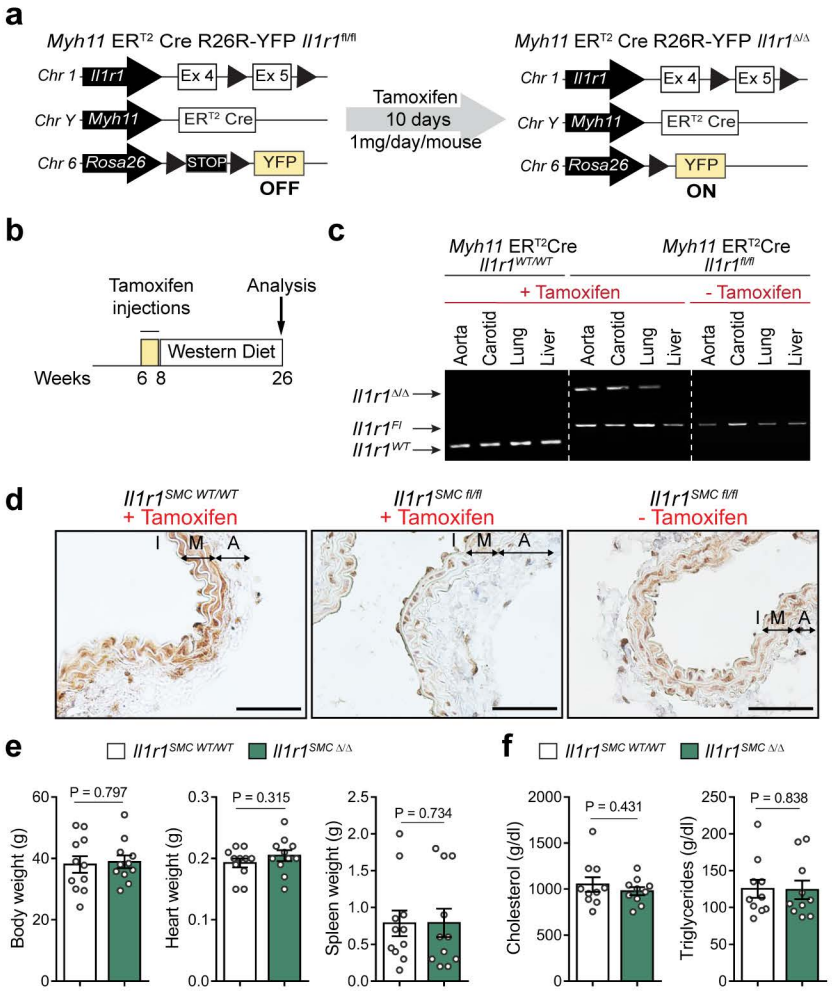

Supplemental Figure 11

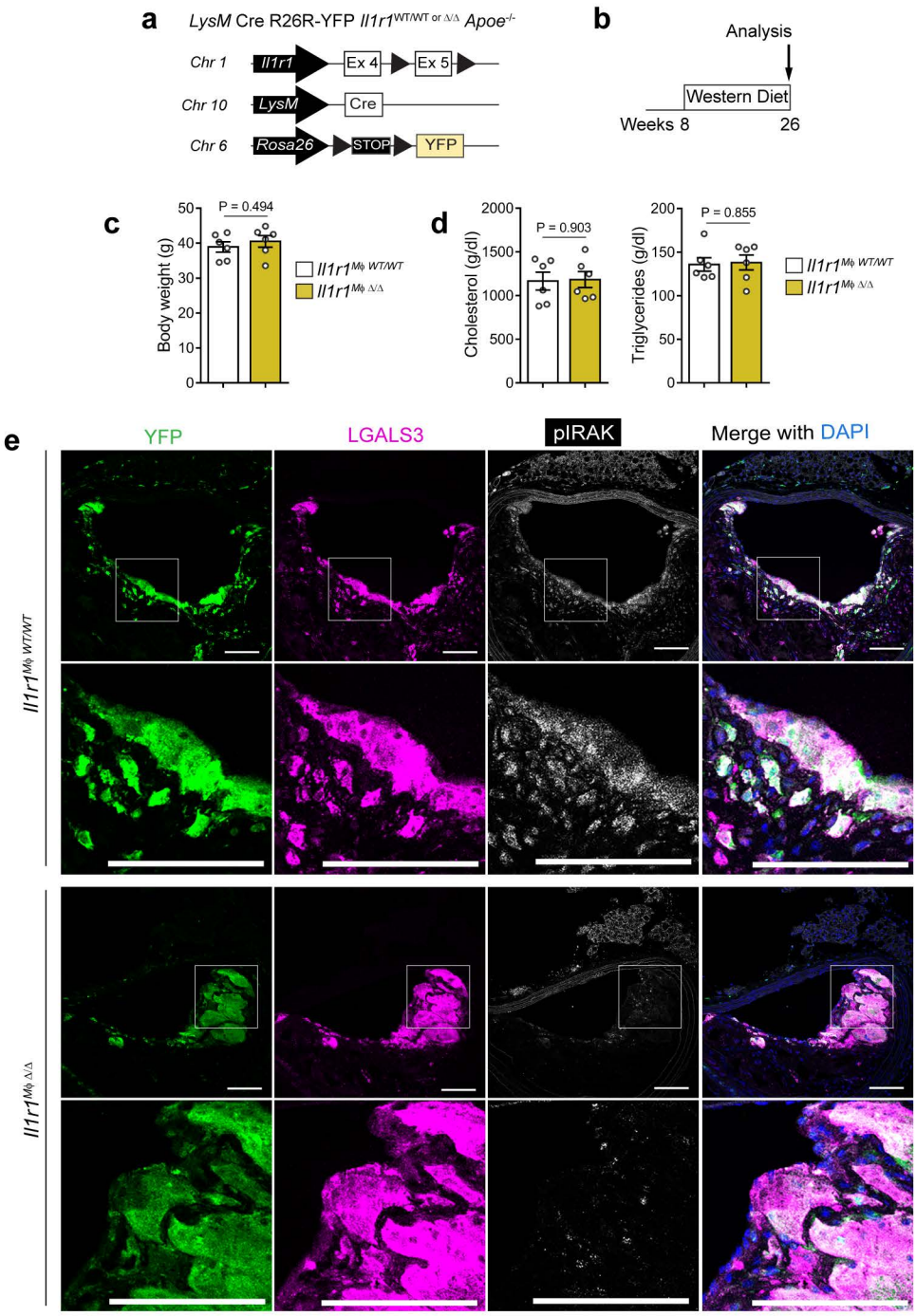

Supplemental Figure 12

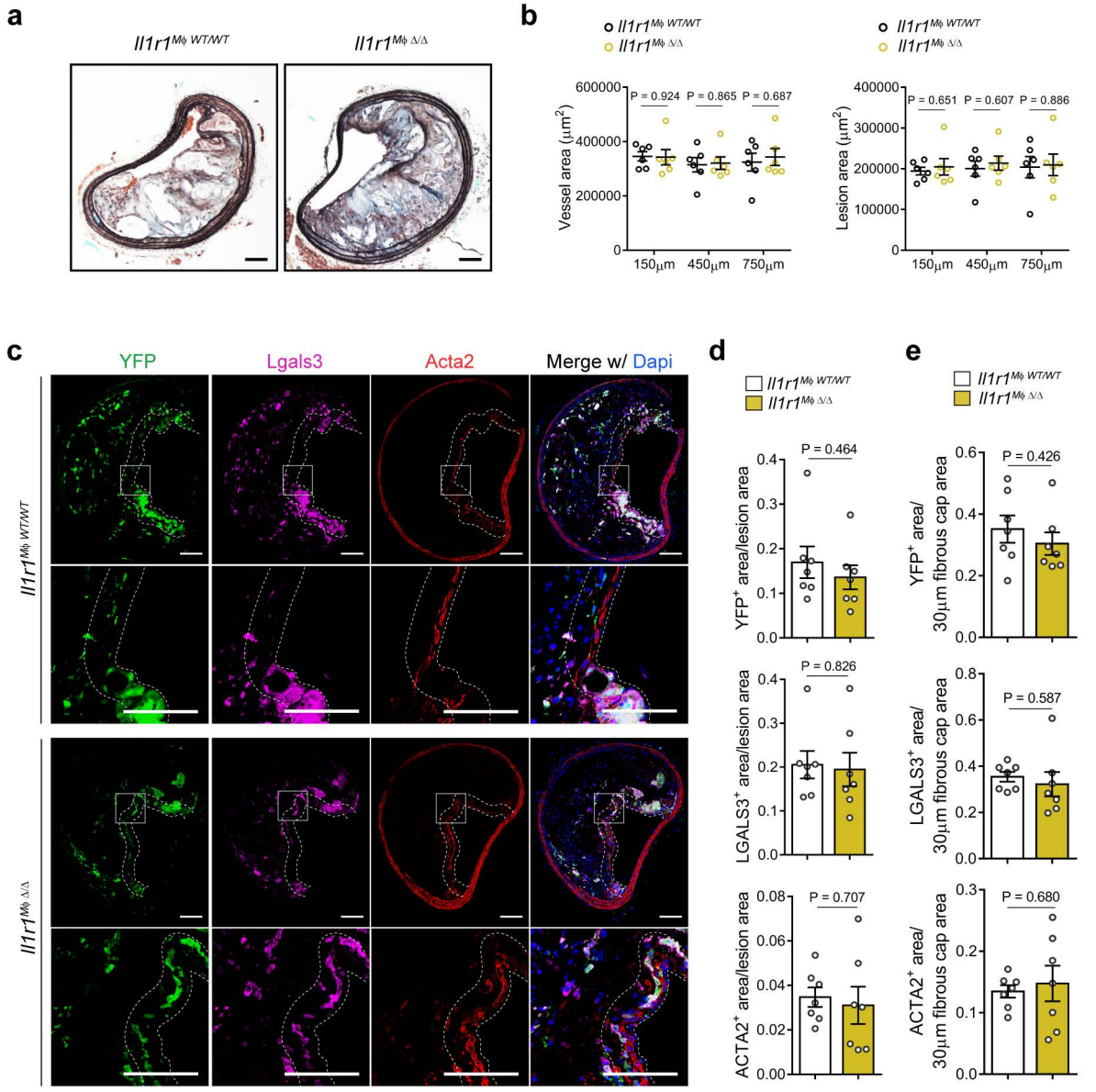

Supplementary information

Supplemental Table 1

Pathways	Fold Difference	p value	Number of genes
mmu03010 Ribosome	-5.989	8.93E-09	88
mmu04380 Osteoclast differentiation	-5.579	3.36E-08	118
mmu04670 Leukocyte transendothelial migration	-4.934	7.66E-07	118
mmu04672 Intestinal immune network for IgA production	-5.125	1.38E-06	43
mmu04621 NOD-like receptor signaling pathway	-4.846	2.13E-06	57
mmu04062 Chemokine signaling pathway	-4.597	3.01E-06	179
mmu04514 Cell adhesion molecules (CAMs)	-4.532	4.54E-06	148
mmu04620 Toll-like receptor signaling pathway	-4.559	4.64E-06	101
mmu04650 Natural killer cell mediated cytotoxicity	-4.490	5.48E-06	124
mmu04662 B cell receptor signaling pathway	-4.542	5.87E-06	75
mmu04612 Antigen processing and presentation	-4.252	1.97E-05	78
mmu04630 Jak-STAT signaling pathway	-4.105	2.60E-05	153
mmu04660 T cell receptor signaling pathway	-4.065	3.39E-05	108
mmu03030 DNA replication	-4.245	3.50E-05	35
mmu04142 Lysosome	-3.994	4.34E-05	122
mmu04666 Fc gamma R-mediated phagocytosis	-3.811	9.59E-05	88
mmu04145 Phagosome	-3.713	1.21E-04	169
mmu04110 Cell cycle	-3.577	2.09E-04	123
mmu04640 Hematopoietic cell lineage	-3.486	3.28E-04	82
mmu04144 Endocytosis	-3.279	5.63E-04	219
mmu04510 Focal adhesion	-3.116	9.82E-04	199
mmu04810 Regulation of actin cytoskeleton	-2.859	2.23E-03	213
mmu04623 Cytosolic DNA-sensing pathway	-2.886	2.37E-03	55
mmu03040 Spliceosome	-2.745	3.30E-03	124
mmu03440 Homologous recombination	-2.821	3.51E-03	27
mmu00190 Oxidative phosphorylation	9.704	3.46E-19	117
mmu00020 Citrate cycle (TCA cycle)	7.090	8.82E-10	31
mmu00280 Valine, leucine and isoleucine degradation	6.367	3.57E-09	49
mmu04146 Peroxisome	5.362	1.44E-07	80
mmu00640 Propanoate metabolism	4.097	6.87E-05	32
mmu00071 Fatty acid metabolism	3.981	7.06E-05	48

mmu04260 Cardiac muscle contraction	3.859	8.78E-05	72
mmu00630 Glyoxylate and dicarboxylate metabolism	3.889	2.16E-04	19
mmu00650 Butanoate metabolism	3.646	2.87E-04	30
mmu03320 PPAR signaling pathway	3.491	3.14E-04	79
mmu00620 Pyruvate metabolism	3.302	7.23E-04	42

Supplemental Table Legends

Supplemental Table 1: RNAseq analysis on BCA tissue extracts reveals downregulation of inflammatory pathways in IL-1β antibody treated mice.

RNAseq analysis of transcript expression in BCA of mice treated with the IL-1β antibody or the IgG control for 8 weeks (n=4 animals per group). Table listing significantly differentially regulated pathways in BCA extracts of mice treated with the IL-1β antibody for 8 weeks as compared to IgG control treated mice, as well as the fold difference, the p value and the number of genes included in each pathway. Significance in differentially expressed genes between IL-1β antibody vs IgG control treated animals was calculated using the DESeq2 Bioconductor R package[1] at a 5% false discovery rate (FDR) ($P_{adj} \leq 0.05$) using the Benjamini–Hochberg procedure to adjust *P* values.

Supplemental Figure Legends

Supplemental Figure 1: Treatment with the IL-1β antibody after 18 weeks of WD decreases in systemic and local inflammation without changing body parameters or lipid profiles.

a – Experimental design of intervention studies in which *Apoe*$^{-/-}$ *Myh11* ER^{T2} Cre YFP mice were fed a WD for 18 weeks and administered 8 weekly injections of IL-1β antibody or IgG control (10 mg/kg). **b** – IL-1β and IL-1α protein levels in plasma and liver. Two-tailed unpaired t-test; mean ± SEM. **c** – Body, heart, and spleen weight in IL-1β antibody and IgG control treated mice (n=12 biologically independent animals per group). **d** – Body weight of mice during the 8 week treatment period (n=9 animals per group). Two-way ANOVA test; mean ± SEM **e** – Plasma cholesterol and triglyceride concentration in IgG control and IL-1β antibody treated mice (n=10 animals per group). Two-tailed unpaired t-test; mean ± SEM. **f** – IgG2a staining in Rag1$^{-/-}$ Apoe$^{-/-}$ mice fed 18 weeks with a WD diet to detect the IL-1β antibody penetration within atherosclerotic lesion (n=3 animals per group). Scale bar: 100µm.

Supplemental Figure 2: Inhibition of IL-1β induces complete inhibition of the outward remodeling in advanced atherosclerotic lesions.

a – Multiple examples of BCA cross-sections stained with Movat from mice treated with IL-1β or and IgG control antibodies. Scale bar, 100 µm. **b-d** – Morphometric analyses of the external elastic lamina (**b**), the internal elastic lamina (**c**), and the lesion area (**d**) at three locations along the BCA (150, 450

and 750 µm from the aortic arch) performed in 26 week WD fed IgG control treated, and 26 week WD fed IL-1β antibody treated *Apoe*$^{-/-}$ *Myh11* ER^{T2} Cre YFP mice (n=13 animal per group). Data were analyzed using a two-way ANOVA and presented as average ± SEM. **e** – Table summarizing the p values of the subsequent ANOVA tests. **f-g** – Quantification of the medial area (**f**) and medial thickness (**g**) in 18 week WD fed, 26 week WD fed IgG control treated, and 26 week WD fed IL-1β antibody treated mice (n=13 animals per group). Data were analyzed using a One-way ANOVA test and presented as the mean ± SEM.

Supplemental Figure 3: IL-1β inhibition is associated with loss of SMC but an increase in the number of macrophage within lesions.

a – Pixel quantification of the YFP^{+}, ACTA2^{+} and LGALS3^{+} area normalized to lesion size (n=9 biologically independent animals per group). **b** – Pixel quantification of the YFP^{+}, ACTA2^{+} and LGALS3^{+} area normalized to the 30µm fibrous cap area (n=16 animals per group). **c** – Single cell counting determining the number of total cells (DAPI), as well as YFP^{+}, LGALS3^{+} and ACTA2^{+} cells normalized to the 30µm fibrous cap area. Results expressed as the number of cells per µm^{2} (n=8 animals per group). **d** – Quantification of YFP^{+}ACTA2^{+} and YFP^{-}ACTA2^{+} cells within the fibrous cap of IL-1β or IgG control antibody treated mice (n=8 animals per group). Data were analyzed using two-tailed unpaired *t*-tests or two-tailed unpaired non-parametric Mann-Whitney tests (mean ± SEM).

Supplemental Figure 4: Treatment with IL-1β antibody is associated with a decrease in collagen content within the fibrous cap but no change the necrotic core size or intraplaque hemorrhage.

a – Schematic of the experimental design. **b** – Representative images of Picrosirius Red staining (bright field, upper panels; polarized light, lower panels). **c** – Quantification of the collagen content in the 30µm fibrous cap area of 18 week WD fed, 26 week WD fed; IgG control treated, and 26 week WD fed; IL-1β antibody treated SMC lineage tracing *Apoe*$^{-/-}$ mice (n=15 animals per group). One-way ANOVA test; mean ± SEM. **d** – Representative images of MMP3 and MMP9 staining. **e** – Quantification of MMP3 (n=11 animals per group) and MMP9 (n=10 animals per group) staining in 26 week WD fed; IgG control treated, and 26 week WD fed; IL-1β antibody treated mice. Two-tailed unpaired t-test; mean ± SEM. **f** – Representative images of Ter119 staining. **g** – Quantification of Ter119^{+} and Ter119^{-} specimen (n=10 animals per group). Two-sided exact Fisher test; percentage of specimen positive and negative for Ter119 staining. **h** – Measurement of the necrotic core size normalized to the lesion size in IL-1β antibody and IgG control treated mice (n=12 animals per group). Two-tailed unpaired t-tests; mean ± SEM. Scale bars, 100 µm (b, d, f).

Supplemental Figure 5: Inhibition of IL-1β in advanced atherosclerotic plaque does not impact lesion calcification.

a – Representative images of Von Kossa staining of non-calcified plaques (upper images) or calcified plaques (lower images) in IgG control and IL-1β treated animals. **b** – Quantification of the percentage of calcified plaques (n=12 animals per group). Data were analyzed using a two-sided exact Fisher test. **c** – Quantification of the proportion of $RUNX2^+$ and YFP^+RUNX2^+ cells normalized to DAPI (n=9 animals per group). Data were analyzed using a two-tailed unpaired *t*-test and were presented as the mean ± SEM. **d** – Representative images of immunostaining for YFP, LGALS3 and RUNX2 in BCA atherosclerotic lesions. Scale bars, 100 µm (**a**,**d**).

Supplemental Figure 6: Comparison of low dose and high dose IL-1β antibody treatment on plaque morphology and cell composition.

a – Schematic representing the experimental design of low and high dose IL-1β antibody treatment for 8 weeks. **b** – Representative images of Movat staining of BCA cross-sections from mice treated with the IgG control (10 mg/kg), the IL-1β antibody at low dose (1 mg/kg), or the IL-1β antibody at high dose (10 mg/kg). **c** – Vessel and lesion size for these three groups (n=13 animals per group). Data were analyzed using a One-way ANOVA; mean ± SEM. **d** – Immunofluorescent staining for YFP, ACTA2 and LGALS3. **e** – Single cell counting for YFP^+, $LGALS3^+$ and YFP^+ACTA2^+ cells within the 30µm fibrous cap area (n=8 animals per group). Counts normalized to DAPI. Data were analyzed using a two-tailed unpaired *t*-test and presented as the mean ± SEM. Scale bars, 100 µm (**b**,**d**).

Supplemental Figure 7: Validation of selective uptake of Cy3-labeled beads by $Ly6C^{low}$ monocytes in monocyte trafficking assays. a - Schematic representing the experimental design of bead uptake assays performed in *Apoe*$^{-/-}$ *Myh11* ER^{T2} Cre YFP mice treated with IL-1β antibody or IgG control. **b** – Gating strategy for determination of monocyte uptake of Cy3-labeled beads. Specifically, dead cells and cell aggregates were removed in (1) and (2). Neutrophils and eosinophils were eliminated using Ly6G and SS Lin (4). Blood monocytes were enriched by CD11b and CD115 gating (3) and (5) and sub-classified by Ly6C expression (6). Endogenous Cy3 bead labeling was readily detectable without amplification (7). **c** – Quantification of the percentage of $CD11b^+$, $Ly6C^{high}$ and $Ly6C^{low}$ cells containing beads 1 day and 21 days after intravenous bead injection (n=6 animals per group). **d** – Quantification of the percentage of $bead^+Ly6C^{low}$ monocytes in IL-1β antibody and IgG control treated mice (n=4 animals per group). **e** – White blood cell count in SMC lineage tracing *Apoe*$^{-/-}$ mice treated for 3 weeks with the IL-1β antibody and IgG control between 18 and 21 weeks of WD (n=5 animals per group). **f** – Red blood cell profile in the same cohort than **e**. Data were analyzed using a two-tailed unpaired *t*-test and presented as the mean ± SEM.

Supplemental Figure 8: Endothelial cell number and proliferation is unchanged after IL-1β inhibition.

a – Single cell counting of $CD31^+$ and $CD31^+Ki67^+$ cells within the 30µm fibrous cap area (n=10 animals per group). Data were analyzed using a two-tailed unpaired *t*-test and presented as the mean ± SEM. **b** – Immunofluorescent staining of CD31, ACTA2 and KI67 in IL-1β Ab and IgG control treated mice. Scale bar, 100µm.

Supplemental Figure 9: Apoptosis assessment by cleaved Caspase 3 staining.

Single cell counting of the total cleaved $Caspase3^+$ cells, cleaved $Caspase3^+YFP^+$ cells, and cleaved $Caspase3^+$ $LGALS3^+$ cells normalized to the total number of cells (DAPI). n=6 animals per group. Data were analyzed using a two-tailed unpaired non-parametric Mann-Whitney test and presented as the mean ± SEM.

Supplemental Figure 10: Validation of SMC-specific *Il1r1* knockout.

a – Schematic representation of the *Myh11* ER^{T2} Cre R26R-YFP $Il1r1^{fl/fl}$ $Apoe^{-/-}$ mouse allowing for tamoxifen-inducible knockout of *Il1r1* in SMC and simultaneous SMC specific lineage tracing. **b** – Schematic of the experimental design showing injection of $Il1r1^{SMC\ fl/fl}$ *and* $^{SMC\ WT/WT}$ mice with tamoxifen daily for 10 days between 6 and 8 weeks of age and subsequently feeding them a WD diet for 18 weeks. **c** – PCR genotyping on several tissues from *Myh11* ER^{T2} Cre R26R-YFP $Il1r1^{WT/WT}$ *and* $Il1r1^{fl/fl}$ demonstrating specific recombination in SMC-rich tissues of the *Il1r1* locus in $Il1r1^{SMC\ fl/fl}$ mice treated with tamoxifen. **d** – Immunostaining for IL1R1 showing specific loss of IL1R1 protein expression in carotid medial layers of $Il1r1^{SMC\ fl/fl}$ mice treated with tamoxifen (I: intima; M: media; A: adventitia). 3 independent repeats. Scale bar, 100 µm. **e-f** – Body parameters (n=11 animals per group) (**e**) and plasma cholesterol and triglyceride concentrations (n=10 animals per group) (**f**) in $Il1r1^{SMC\ fl/fl}$ *and* $^{SMC\ WT/WT}$ mice after 18 weeks of WD. Data were analyzed using two-tailed unpaired *t*-tests or two-tailed unpaired non-parametric Mann-Whitney tests. Mean ± SEM.

Supplemental Figure 11: Validation of macrophage-selective *Il1r1* knockout.

a – Schematic representation of the *LysM* Cre R26R-YFP $Il1r1^{fl/fl}$ $Apoe^{-/-}$ mouse allowing conditional, non-inducible knockout of *Il1r1* and simultaneous lineage tracing of LysM expressing cells. **b** – Schematic of the experimental design showing MΦ-*Il1r1* mice fed a WD diet for 18 weeks. **c** – Body weight of $Il1r1^{MΦ\ WT/WT}$ and $Il1r1^{MΦΔ/Δ}$ after 18 weeks of WD (n=6 animals per group). **d** – Plasma cholesterol and lipid concentration of MΦ-*Il1r1* mice after 18 weeks of WD (n=6 animals per group). **e** – Immunofluorescent staining of phospho-IRAK in BCA cross-sections of $Il1r1^{MΦ\ WT/WT}$ and $Il1r1^{MΦΔ/Δ}$ after

18 weeks of WD demonstrating that *Il1r1*$^{M\Phi\Delta/\Delta}$ have a complete loss of IL-1 signaling in YFP^{+}LGALS3^{+} macrophages (n=6 animals per group). Scale bar, 100 µm.

Supplemental Figure 12: Macrophage-selective *Il1r1* KO does not induce changes in atherosclerotic lesion development. a – Representative images of Movat staining of BCA cross-sections. **b** – Vessel and lesion area at three locations of the BCA (distance from the aortic arch) in *Il1r1*$^{M\Phi\ \Delta/\Delta}$ and littermate controls (n=6 per group). **c** – Immunofluorescent staining for YFP, LGALS3, and ACTA2 of BCA sections from MΦ-*Il1r1* mice. Scale bar, 100 µm. **d** – Quantification of the YFP^{+}, LGALS3^{+}, and ACTA2^{+} area normalized to the lesion in *Il1r1*$^{M\Phi\ \Delta/\Delta}$ and littermate controls (n=7 per group). **e** – Quantification of the YFP^{+}, LGALS3^{+}, and ACTA2^{+} area normalized to the 30µm fibrous cap area in *Il1r1*$^{M\Phi\ \Delta/\Delta}$ and littermate controls. Data were analyzed using two-tailed unpaired *t*-tests or one-way ANOVA (**b**) and presented as the mean ± SEM.

References

1 Love, M. I., Huber, W. & Anders, S. Moderated estimation of fold change and dispersion for RNA-seq data with DESeq2. *Genome Biol* **15**, 550, doi:10.1186/s13059-014-0550-8 (2014).